The ISME Journal (2011) 5, 1484–1493
© 2011 International Society for Microbial Ecology All rights reserved 1751-7362/11
www.nature.com/ismej

Open

ORIGINAL ARTICLE

Nitrogen fixation and transfer in open ocean diatom–cyanobacterial symbioses

Rachel A Foster[1,2], Marcel MM Kuypers[2], Tomas Vagner[2], Ryan W Paerl[1], Niculina Musat[2] and Jonathan P Zehr[1]

[1]*Ocean Sciences Department, University of California, Santa Cruz, CA, USA and* [2]*Department of Biogeochemistry, Max Planck Institute for Marine Microbiology, Bremen, Germany*

Many diatoms that inhabit low-nutrient waters of the open ocean live in close association with cyanobacteria. Some of these associations are believed to be mutualistic, where N_2-fixing cyanobacterial symbionts provide N for the diatoms. Rates of N_2 fixation by symbiotic cyanobacteria and the N transfer to their diatom partners were measured using a high-resolution nanometer scale secondary ion mass spectrometry approach in natural populations. Cell-specific rates of N_2 fixation (1.15–71.5 fmol N per cell h^{-1}) were similar amongst the symbioses and rapid transfer (within 30 min) of fixed N was also measured. Similar growth rates for the diatoms and their symbionts were determined and the symbiotic growth rates were higher than those estimated for free-living cells. The N_2 fixation rates estimated for *Richelia* and *Calothrix* symbionts were 171–420 times higher when the cells were symbiotic compared with the rates estimated for the cells living freely. When combined, the latter two results suggest that the diatom partners influence the growth and metabolism of their cyanobacterial symbionts. We estimated that *Richelia* fix 81–744% more N than needed for their own growth and up to 97.3% of the fixed N is transferred to the diatom partners. This study provides new information on the mechanisms controlling N input into the open ocean by symbiotic microorganisms, which are widespread and important for oceanic primary production. Further, this is the first demonstration of N transfer from an N_2 fixer to a unicellular partner. These symbioses are important models for molecular regulation and nutrient exchange in symbiotic systems.
The ISME Journal (2011) **5,** 1484–1493; doi:10.1038/ismej.2011.26; published online 31 March 2011
Subject Category: microbe–microbe and microbe–host interactions
Keywords: nanoSIMS; symbioses; cyanobiont; diatoms; N_2 fixation

Introduction

It is well established that oceanic N_2 fixation has a pivotal role in providing 'fixed' nitrogen (N; new production) to surface water communities (Karl *et al.*, 1997, 2002). However, there is a continuing controversy regarding the apparent imbalance in the sources and sinks of N in the global N budget (Codispoti, 1995; Michaels *et al.*, 1996; Gruber, 2005). Many studies over the last decade have shown the presence and activity of diverse N_2-fixing microorganisms (Zehr *et al.*, 1998, 2000; Montoya *et al.*, 2004), and so it has also been argued that N input from these other N_2-fixing microorganisms (that is, unicellular groups) have been underestimated. Furthermore, there is new evidence strongly suggesting a methodological underestimation of oceanic N_2 fixation rates by standard isotope tracer experiments (Mohr *et al.*, 2010). A unique group of open ocean diazotrophs, which have been understudied, including their N_2-fixing activities, are the heterocystous cyanobacteria that live symbiotically with other phytoplankton, primarily diatoms.

Richelia intracellularis and *Calothrix rhizosoleniae* are filamentous heterocystous cyanobacteria that live in presumed symbioses with several diatom genera, including *Hemiaulus*, *Rhizosolenia* and *Chaetoceros* (Figures 1a–c; see also illustrations of diatom ultrastructure in Tomas, 1997). Heterocysts are specialized cells in which N_2 fixation is localized (Stewart, 1973), and therefore it is assumed that the cyanobacterial symbionts provide fixed N to the diatom partners. *Richelia* spp. and *Calothrix* spp. have morphologically similar filaments, called trichomes, comprised of vegetative cells and a terminal heterocyst. The length, location and number of *Richelia* and *Calothrix* trichomes per diatom partner, and phylogeny of the symbionts differ in each symbiosis (Janson *et al.*, 1999; Foster and Zehr, 2006). There is another less studied symbiosis between the chain-forming pennate diatom, *Climacodium frauenfeldianum* and unicellular cyanobacteria similar in morphology to the free-living diazotroph, *Crocosphaera watsonii* (Figure 1d). A recent re-evaluation of the partial

Correspondence: R Foster, Department of Biogeochemistry, Max Planck Institute for Marine Microbiology, Celsiusst. 1, MPI for Marine Microbiology, D-28359 Bremen, Germany.
E-mail: rfoster@mpi-bremen.de
Received 16 November 2010; revised 8 February 2011; accepted 8 February 2011; published online 31 March 2011

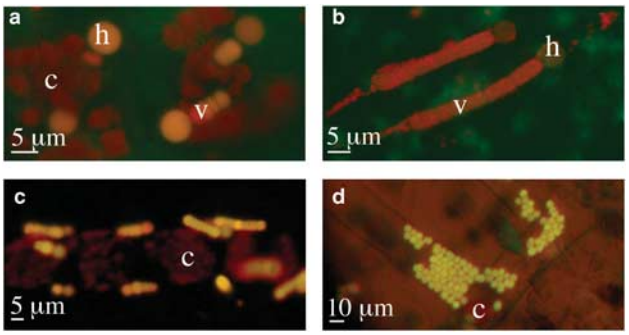

Figure 1 Blue light excitation (450–490 nm) images of field collected diatom–cyanobacteria symbioses. The diatom frustules are not easily seen under epi-fluorescence microscopy (except in **d**), however, the excitation patterns of the cyanobacterial symbionts are clearly different and yellow/orange from their diatom partners (red). (**a**) Two *Hemiaulus membranaceus* diatoms with two *Richelia intracellularis* associated to each diatom. The chlorophyll a within the chloroplast (c) of the diatom fluoresces red, whereas the pigments in the vegetative (v) cells and the terminal heterocyst (h) of *Richelia* fluoresce yellow–orange. (**b**) The apical end of a *Rhizosolenia clevei* diatom with two associated trichomes of *R. intracellularis* (**c**) A chain of *Chaetoceros* spp. diatoms with *Calothrix rhizosoleniae* attached to the spines (not visible). (**d**) A chain of *Climacodium frauenfeldianum* diatoms associated with yellow-fluorescing unicellular cyanobacteria (cyanobionts).

16S rRNA sequence derived from a symbiotic *C. frauenfeldianum* reported by Carpenter and Janson (2000), found 100% sequence identity to *C. watsonii* 8501 (personal communication, Shellie Bench). The benefit (or costs) of the symbiotic relationship for either partner has not been clearly characterized in any of the diatom–cyanobacterial symbioses, but a primary interaction has been assumed to be provision of fixed N to the diatom by the potentially N_2-fixing symbiont.

The symbiotic diatoms have been observed in all the major ocean basins (see review, Foster and O'Mullan 2008), where bloom cell densities have been reported (Villareal, 1994; Carpenter *et al.*, 1999), however, there are few reported N_2 (and carbon (C)) fixation rate measurements for the symbiotic populations. Of the few reported rate measures, estimates were determined from bulk water assays or cell concentrates (plankton slurries) and therefore, the rate estimates include N_2 fixation by other co-existing populations, such as *Trichodesmium* and unicellular cyanobacteria. Recent methodological advancements have made it possible to directly measure and visualize stable isotopes in individual cells (Römer *et al.*, 2006; Clode *et al.*, 2007; Lechene *et al.*, 2007; Ropa *et al.*, 2007; Musat *et al.*, 2008; Finzi-Hart *et al.*, 2009; Halm *et al.*, 2009; Ploug *et al.*, 2010). Using a high-resolution nanometer scale secondary ion mass spectrometry (NanoSIMS; Cameca, Gennevilliers Cedex, France) approach we provide the first experimental evidence of N_2 fixation and transfer of fixed N products in field populations of symbiotic diatoms.

Materials and methods

$^{15}N_2$ incubations

Two sets of long-term incubation (0, 24, 48 and 76 h) experiments were run in July 2008 at two locations in the Gulf of California (21 23 °N, 107.05 °W and 24 49 °N, 109 00 °W) and one location in the subtropical North Pacific (24 4 °N, 158 27.96 °W). In July 2009, one short-term (0, 30 min, 1, 3 and 12 h) set of experiments was performed at the same location of the subtropical North Pacific. Bulk seawater (SW) was collected from 0 to 10 m using a conductivity temperature depth (CTD) rosette connected to a hydro wire. The 0–10 m depth was selected, as this was the depth where the most symbiotic diatoms were observed with microscopy.

In July 2008, two experimental designs were used, in which in one design, 4.4 l bottles were filled with bulk SW from the CTD, capped and sealed without air bubbles, and subsequently amended with 3 ml of $^{15}N_2$ (98% + $^{15}N_2$, Cambridge isotopes). In the second design, 5 l of bulk SW was gravity filtered, and the >5 μm cell diameter concentrates were incubated with 200 ml filtered SW, capped, sealed as described above, and amended with 150 μl of $^{15}N_2$. This latter design was used to decrease the time of filtration at the subsequent time points. In July 2009, only 4.4 l bottles were used and treated as described above. All incubations were held at ambient sea surface temperatures by continuously flowing SW and 50% incident surface irradiance.

At the time of injection (time 0), and at the subsequent time points, the entire contents of incubation bottles were filtered onto a membrane filter using a peristaltic pump and fixed overnight at 4 °C in (w/v) 100 μl of 4% paraformaldehyde. The July 2008 long-term experiments used 3 or 10 μm pore size filters and the July 2009 short-term experiments used 3.0 μm pore size filters, which were pre-sputtered with gold (Au) and palladium (Pd). Filters were washed three times in 0.1 M phosphate-buffered saline and stored dry at −20 °C.

NanoSIMS analyses

Cells from the July 2008 experiments were re-suspended from the 3.0 μm pore size membrane filters by gentle pippeting, then filtered onto a 3.0 μm pore size Au–Pd sputtered membrane filter and washed with 15 ml of Milli-Q water. This step was omitted for the July 2009 filters, as these were filtered directly onto pre-sputtered filters. A 5 mm diameter circle was excised in the area on the filter comprised of a few (that is, >3 symbioses) symbiotic diatoms and/or free-living cells. Epi-fluorescent images of each free-living cell and diatom-containing symbionts were taken before the nanoSIMS analyses. Once dried, the filters were scanned for diatoms containing *Richelia*/*Calothrix* and *Climacodium* cells with *Crocosphaera* symbionts, and in

addition, free-living cells of *Richelia*, *Calothrix* and *Crocosphaera* were also identified using a Zeiss Axioplan (Zeiss, Jena, Germany) epi-fluorescent microscope fitted with blue (450–490 nm) and green (510–560 nm) excitation filters. All cells were identified by shape, cell diameter and excitation patterns. In addition, the taper of the trichome was also used to distinguish the *Richelia* and *Calothrix* symbionts. Given the 100% 16S rRNA sequence identity between *C. watsonii* 8501 and the partial sequences reported previously from symbiotic *Climacodium* diatoms (Carpenter and Janson, 2000), we assumed that the unicellular symbionts were *Crocosphaera*.

For each time point of the long-term incubations (0–76 h), two to three different *Hemiaulus–Richelia* symbioses were analyzed. For the *Climacodium* and *Chaetoceros* diatoms containing symbionts, cells were only re-identified at the initial time (time 0) and at 76 h time points. We were not able to find these latter symbioses in the 24 and 48 h time point samples in the long-term experiments of July 2008. Only *Hemiaulus–Richelia* symbioses, and free-living *Calothrix* and *Richelia* (from time points 1 and 12 h, respectively) cells were analyzed in the short-term experiments of July 2009 as these were consistently observed with microscopy. In addition, a large group (19 cells) of *Crocosphaera* cells were also analyzed from the 12 h time point sample to provide a comparison measure for the *Crocosphaera* cells living symbiotically with *Climacodium*. The number of cell replicates for analysis at each time point was limited by the low cell abundances of the symbioses and free-living cells (*Richelia*, *Calothrix* and *Crocosphaera*) at the time of collection. Multiple planes (>50) were recorded to assure a considerable robustness of the single-cell rate measurements.

NanoSIMS analysis was performed using a Cameca NanoSIMS 50 l instrument following previously described methods (Musat *et al.*, 2008). Briefly, samples were rastered with 16 keV Cesium (Cs^+) primary ions with current between 1–3 pA. Primary ions were focused into nominal $\sim$120 nm spot diameter. Mass resolving power in all measurements was >6000. The primary ion beam was used to raster the analyzed area with 256×256 pixels over the chosen raster size with dwelling time 1 or 2 ms per pixel. Negative secondary ions were collected simultaneously in electron multiplier detectors.

All scans were corrected for drift of the beam and sample stage after acquisition. Isotope ratio image was created as ratio of a sum of total counts for each pixel over all recorded planes of the investigated isotope and the main isotope. Regions of interest (ROI) around cell structures were defined using the parallel epi-fluorescent image taken before nanoSIMS analyses together with secondary ion images. For each ROI, the ratios $^{15}N/^{14}N$ (for example, inferred from $^{12}C^{15}N/^{12}C^{14}N$) were calculated.

Calculations: biovolume, ^{15}N assimilation rates, %N transfer, growth rate, excess N assimilation, global N contribution

Epi-fluorescent images taken before nanoSIMS analyses were used with Axioscope software (Zeiss Axiovision Rel 4.7.2, Zeiss) to estimate heterocyst and unicellular cyanobiont cell diameters, and the apical and trans-apical dimensions of the *Hemiaulus* diatoms. As the cells were fixed and dried to the filters and the depth (Z plane) was not visible under the microscope, we assumed that the height of the *Hemiaulus, Chaetoceros* and *Climacodium* cells was the same as the diameter of their respective symbiont's heterocyst or unicellular cell diameter.

Measurements of cell diameter, apical and trans-apical axes for the *Hemiaulus* and *Chaetoceros* cells were used in a biovolume estimate for an elliptic prism and four cones (23-SL) and a prism on an elliptic base (29-H) as described by Sun and Liu (2003). Similar measures for the *Climacodium* cells were made in a biovolume estimate for a box plus a prism on a triangle base (30-H; Sun and Liu, 2003). The volume for the *Crocosphaera* cells (free-living and symbiotic) and the vegetative and heterocyst cells of *Richelia* and *Calothrix* was estimated by using the equation for a sphere (Sun and Liu, 2003). C content was calculated for the diatoms and symbionts, using the Strathmann (1967) equations, where the biovolume (V) was used in place of plasma volume. The C content was then used to estimate nitrogen (N) content by assuming a Redfield ratio of 6.6 (Redfield, 1934). As none of the symbiotic diatoms have been brought into pure culture, and at the time of our incubations cell densities were too low for standard elemental analysis, we considered our estimate of the initial N content based on biovolume and Redfield ratio as conservative and a reasonable alternative.

Nitrogen assimilation for individual symbiotic cells (fmol N per cell) were estimated by: assimilation $= [^{15}N_{ex} \times N_{con}]/N_{sr}$. The $^{15}N_{ex}$ is the mean of the $^{15}N/^{14}N$ ratios of the individual ROIs from the diatoms corrected for by the mean value of the $^{15}N/^{14}N$ ratios in diatoms of the time zero samples and divided by 100; the N_{con} is the N content estimated by V and the Strathmann (1967) equations as described above, and N_{sr} is the calculated atom percent (AT%) of ^{15}N in the experimental bottle according to Zehr and Montoya (2007). The assimilated N was divided by incubation time to determine cell-specific N_2 fixation rates (fmol N per cell h^{-1}).

The percentage of fixed N transferred to the diatom partners was determined by dividing the N assimilated as calculated above by the sum of N assimilated into the diatom, vegetative cells and heterocysts and multiplying by 100. Growth rate for the symbionts and diatom partners were estimated by the following, $V = 1/t\ (R_{(F)} - R_{(I)}/R_{(S)} - R_{(I)})$, where t is time, the $R_{(F)}$ is estimated from mean value of the ROIs (for diatom and symbiont separately) at

specific time points, the $R_{(I)}$ is the mean AT% of the ROIs for the diatom or symbiont in the time zero samples, and the $R_{(S)}$ is the calculated AT% of ^{15}N in the experimental bottle according to Zehr and Montoya (2007).

To determine the percent of N fixed by the *Richelia* that was in excess of their own growth requirement and the percent of the diatom partner's growth supported by *Richelia*, we assumed growth rates for *Hemiaulus* and *Richelia* to be equivalent to that reported by Villareal (1989, 1990). These were 0.77 and 0.67 division per day, respectively, and we converted these to specific growth rate, K', by $K' = \text{division per day} \times \text{Ln2}$. These assumed values were also within the range we estimated for growth of both the *Richelia* and the *Hemaiulus*, which is described above (Table 1). We estimated the percent of the diatom's growth requirement supported by the *Richelia* by the following, $(\text{assimilation}/(N_{con} \times K')) \times 100$, where assimilation is estimated as described above, N_{con} is N content estimated from *V* and Strathmann (1967) equations, and K' is the assumed growth rate. The percentage of excess N fixed by the *Richelia* was calculated by the total N assimilated (host, vegetative cells and heterocysts) normalized to incubation time divided by the N_{con} of the symbiont multiplied by assumed growth rate (0.67 division per day).

Table 1 Summary of nanoSIMS analyses, cell dimensions and estimates of N_2 fixation rates and growth rates

Diatom symbiont	*Time (h)*	*ROIs (n)*	*AT % ($^{15}N/^{14}N$)*	*Biovolume (μm^3)*	*N_2 fix rate (fmol N per cell h^{-1})*[a]	*Growth rate (division per day)*
Hemiaulus		3	0.3789	4.22×10^3		0.22
Heterocyst 1		1	0.3726	164	21.0	
Vegetative	0.5	1	0.3790	8.72		0.22
Heterocyst 2		1	0.3812	37.4		
Vegetative		1	0.3806	16.4		0.23
Hemiaulus		3	0.3651	3.49×10^3		0.06
Heterocyst	1	1	0.3761	102	5.88	
Vegetative		2	0.3607	8.32		0.05
Hemiaulus		4	0.3759	1.87×10^3		0.10
Heterocyst	1	1	0.3764	85.1	8.94	
Vegetative		2	0.3737	15.5		0.09
Hemiaulus			0.3595	1.91×10^3		0.03
Heterocyst	1	1	0.3623	34.3	2.90	
Vegetative		2	0.3657	8.62		0.06
Hemiaulus		6	0.4378	4.63×10^3		0.11
Heterocyst		1	0.4238	50.0	9.45	
Vegetative	3	3	0.4362	6.0		
Heterocyst		1	0.4508	45.6		0.10
Hemiaulus		8	0.4576	4.23×10^3		0.13
Heterocyst 1	3	1	0.4104	72.3	10.6	
Vegetative		2	0.4792	29.6		0.16
Heterocyst 2		1	0.4706	44.9		
Hemiaulus		6	0.4523	4.32×10^3		0.12
Heterocyst 1		1	0.4118	41.1		
Vegetative	3	1	0.4951	11.7	10.3	0.10
Heterocyst 2		1	0.4596	55.0		
Vegetative		1	0.4485	13.4		0.11
Hemiaulus	12	5	0.4739	1.56×10^3		0.04
Heterocyst		1	0.4572	13.1	1.41	
Hemiaulus		5	0.4519	1.49×10^3		0.04
Heterocyst	12	1	0.4826	10.4	1.15	
Vegetative		2	0.4748	5.77		0.04
FL Calothrix						
Heterocyst	1	1	0.3570	35.8	0.17	0.06
Vgetative		6	0.3679	28.5		
FL Richelia						
Heterocyst	12	1	0.4575	44.5	0.12	
Vegetative		6	0.7415	45.1		0.11
FL Crocosphaera	12	19	0.3561–0.4519	$65–2.66 \times 10^2$	0.02–2.39	0.001–0.15

Table 1 (Continued)

Diatom symbiont	*Time (h)*	*ROIs (n)*	*AT % ($^{15}N/^{14}N$)*	*Biovolume (μm^3)*	*N_2 fix rate (fmol N per cell h^{-1})*[a]	*Growth rate (division per day)*
Hemiaulus		3	0.4032	2.39×10^4		
Heterocyst 1	0	1	0.3632	9.10×10^2		
Heterocyst 2		1	0.3951	3.17×10^2		
Hemiaulus		3	0.3494	2.84×10^4		
Heterocyst 1		1	0.3689	6.84×10^2		
Heterocyst 2	0	1	0.3743	4.37×10^2		
vegetative		1	0.3617	2.34×10^2		
Hemiaulus		4	4.4440	4.41×10^3		0.43
Heterocyst	24	1	1.7900	75.3	47.8	
Vegetative		2	4.4600	18.9		0.43
Hemiaulus		3	4.6600	3.12×10^3		0.45
Heterocyst	24	1	2.6810	71.0	38.7	
Vegetative		3	4.7430	27.4		0.46
Hemiaulus		6	4.5960	4.31×10^3		0.45
Heterocyst 1		1	4.7068	38.7	48.7	
Vegetative	24	1	4.7815	7.37		0.47
Heterocyst 2		1	4.9327	48.6		
Vegetative		2	4.9693	28.8		0.49
Hemiaulus		4	3.1628	2.12×10^3		0.15
heterocyst 1		1	3.1141	39.1	9.43	
vegetative	48	2	3.8720	41.6		0.18
heterocyst 2		1	3.9909	35.8		
Hemiaulus		3	3.0170	4.30×10^3		0.14
Heterocyst	48	1	3.4009	41.9	15.3	
Vegetative		4	3.5284	23.4		0.17
Hemiaulus		3	3.0506	4.68×10^3		0.14
Heterocyst	48	1	3.6647	12.1×10^1	16.5	
Vegetative		3	3.5281	16.6		0.33
Hemiaulus		4	9.7529	4.40×10^3		0.48
Heterocyst 1		1	9.8114	74.0	50.4	
Vegetative	76	1	10.655	14.0		0.48
Heterocyst 2		1	11.652	68.9		
Vegetative		1	11.891	33.2		0.59
Hemiaulus		3	9.6706	4.33×10^3		0.48
Heterocyst	76	1	3.1086	94.8	49.2	
Vegetative		1	9.0384	41.6		0.44
Chaetoceros		12	0.3593	nm		
Heterocyst 1		1	0.3056	11.9		
Vegetative	0	13	0.3339	29.6		
Heterocyst 2		1	0.3417	15.6		
Vegetative		5	0.3398	44.0		
Chaetoceros		3	7.6500	2.17×10^4		0.38
Heterocyst 1		1	4.3552	91.3	71.5	
Vegetative	76	3	7.0634	67.0		0.35
Heterocyst 2		1	6.5394	70.9		
Vegetative		10	6.9387	66.7		0.32
Climacodium	0	2	0.3797	nm		
Crocosphaera		4	0.3710	55.9		
Climacodium	76	11	3.1657	1.56×10^5	6.03	0.37
Crocosphaera		28	5.3341	65.4	1.62	0.26

Abbreviations: AT%, atom percent; FL, free living (non-symbiotic); nanoSIMS, nanometer scale secondary ion mass spectrometry; nm, not measured; ROIs, regions of interests.
[a]N_2 fixation rates were normalized by number of N_2-fixing cell.

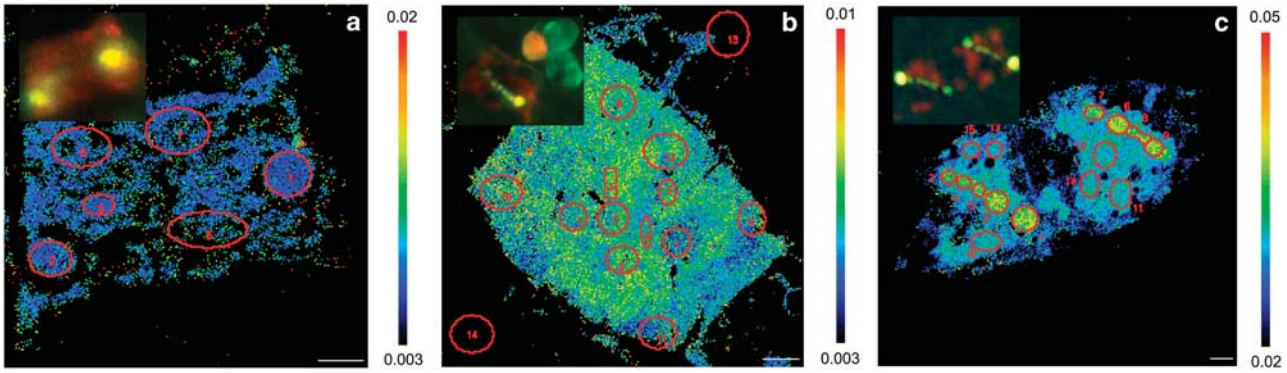

Figure 2 The images of $^{15}N/^{14}N$ ratios are shown for symbiont-containing *Hemiaulus*. The $^{15}N/^{14}N$ ratio is shown for *Hemiaulus–Richelia* symbioses at time 0 (**a**), 30 min (**b**) and 48 h (**c**). Inset panels **a–c** are the epi-fluorescent images taken before the nanoSIMS analyses. The numbers and markings in the figure define regions of interest, which were used for calculating $^{15}N/^{14}N$ ratios. Scale bars are 5 μm.

To estimate the contribution of the various symbiotic diatoms to basin scale N_2 assimilation, we used non-bloom cell abundances reported for the Atlantic (39 cells l^{-1}; Carpenter *et al.*, 1999) and the Pacific (80 cells l^{-1}, Venrick 1974; Mague *et al.*, 1974), the range in N_2 assimilation determined from our nanoSIMS analyses of all the symbiotic cells, a domain of 17.8 and 27.8 $km^2 \times 10^6$ for the Atlantic and Pacific Oceans, respectively (Gruber and Sarmiento, 1997; Mahaffey *et al.*, 2005; Carpenter and Capone, 2008), and 365 days of activity (12 h per day) to a depth of 10 m.

Results and discussion

Bulk SW samples from two regions of the Pacific Ocean were incubated with $^{15}N_2$ to trace and quantify the N_2 fixation by cyanobacterial symbionts of various diatom genera at the cellular level. As diatoms are not able to acquire N from N_2, they rely on extracellular dissolved fixed inorganic nitrogen pools (nitrate and ammonium), which in the open ocean surface waters are present at extremely low concentrations. Thus, the diatoms housing symbiotic diazotrophs have a distinct advantage if they can acquire the N_2 fixed by their cyanobacterial partners. The nanoSIMS approach made it possible to visualize and quantify the ^{15}N fixed in the symbionts and transferred to the diatom cells (Figures 2 and 3). In addition, the cyanobacterial partners were fully supporting the diatom N requirements for growth, as we always observed equal or higher enrichment in the diatoms than in the vegetative cells.

In the initial set of experiments, the ^{15}N enrichment pattern within a chain of *Hemiaulus* cells clearly mirrored the location of two associated *Richelia* trichomes imaged before the analyses with epifluorescence microscopy (Figure 2), showing that the cyanobacteria fixed N. In addition, in areas identified as the diatom chloroplasts (that is, excited red in the epi-fluorescence image) were also enriched, suggesting that N was transferred from symbiont to diatom partner. Similarly, substantial ^{15}N labeling was observed in the *Calothrix* heterocyst and vegetative cells and also in the *Chaetoceros* diatoms, suggesting that N was transferred along the trichome of the symbiont, and in addition, across the cell membrane of the diatom partner (Figure 3a). The ^{15}N enrichment was most obvious in <1 μm diameter 'hotspots' inside the *Crocosphaera* cells found associated with the *Climacodium* diatoms (Figure 3c). In the *Chaetoceros* and *Climacodium* symbioses N_2 fixation had not been previously demonstrated. In general, the transfer of fixed N to the diatom partners in all of the diatom–cyanobacterial symbioses had previously been assumed and had never been demonstrated. The nanoSIMS results directly prove that the N_2-fixing cyanobionts provide fixed N to their diatom partners.

The transfer and incorporation of N from the cyanobacteria to the diatom cells was faster than the length of the sampling period in the initial set of experiments (24–76 h). Diatoms, and other cells in oligotrophic oceans are often assumed to grow slowly due to low ambient nutrient concentrations, and thus we anticipated that the symbiont would only transfer a fraction of the N_2 fixed to the diatom partner within the incubation. However, in our long-term experiments, the enrichment was high after 24 h (Figure 4a) and we were not able to estimate the N transfer over the shorter time interval. In our subsequent short-term experiments, we observed elevated ^{15}N enrichment in *Hemiaulus* cells incubated for as short as 30 min and as the range of enrichment was similar in the cells measured after 3 and 12 h incubations, it appears that N transfer saturated by 3 h (Figure 4b). The near saturation within 3 h was much faster than anticipated, and means that measured fixation rates may be underestimated. We expected that the transfer would be slow, as the symbionts reside external to the diatom cell membrane. The *Richelia* symbionts reside between the frustule and the cell membrane (plasmalemma) of the *Hemiaulus* diatom cell wall (Janson *et al.*, 1995), whereas the *Calothrix* symbionts are extracellular on the *Chaetoceros* diatom

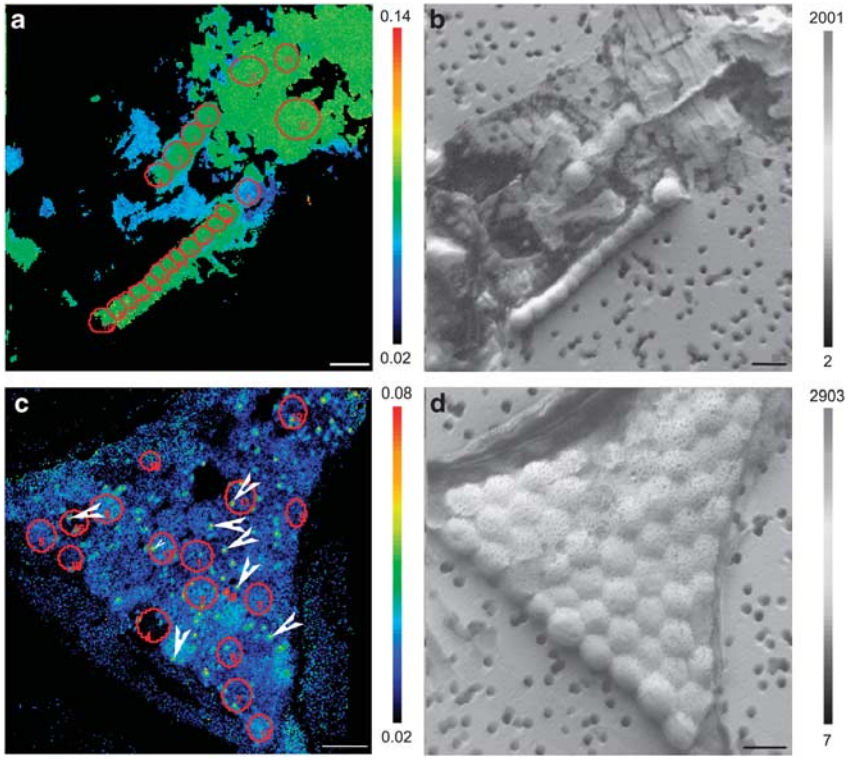

Figure 3 The images of $^{15}N/^{14}N$ ratios are shown for *Chaetoceros-Calothrix* and the *Climacodium*-cyanobiont symbioses. The $^{15}N/^{14}N$ ratio is shown in A and C for *Chaetoceros–Calothrix* and the *Climacodium–Crocosphaera* symbioses, respectively. Note the 'hotspots' (white arrows) of enrichment within the individual cyanobiont (*Crocosphaera*) cells of *Climacodium* (**c**). The corresponding total ion content images images for the same symbioses in **a** and **c** are shown in **b** and **d**, respectively. The numbers and markings in the Figure define regions of interest, which were used for calculating $^{15}N/^{14}N$ ratios. Scale bars are 5 μm.

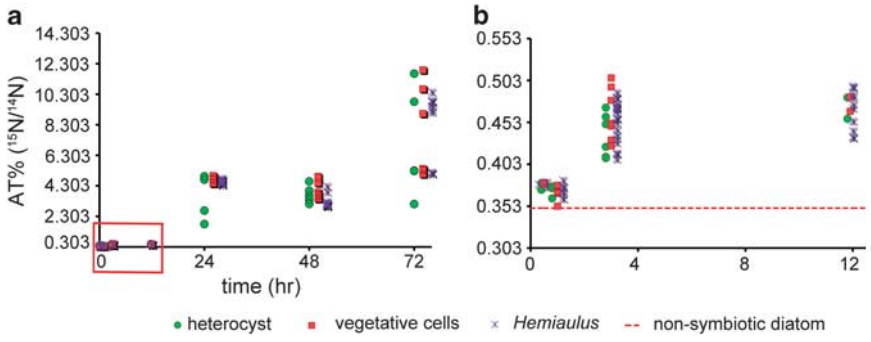

Figure 4 Summary of results from nanoSIMS analysis. (**a**) The atom % of the $^{15}N/^{14}N$ ratios for ROIs of individual *Hemiaulus–Richelia* are shown as a function of incubation time in both long and short-term experiments. (**b**) The atom % of the $^{15}N/^{14}N$ ratios for ROIs of individual *Hemiaulus–Richelia* symbioses from the short-term experiments and represents the values within the red box shown in **a**. Note that the *Richelia* enrichment values are given as ratios estimated in the heterocyst and the vegetative cells. The dashed red line indicates the value for a co-occurring non-symbiotic diatom.

(Norris, 1961), and the cyanobiont (*Crocosphaera*) location is unknown in the *Climacodium* symbioses. The N transfer we observed along the trichomes of symbiotic and free-living *Richelia* and *Calothrix* was not unexpected, as rapid transfer has already been reported for lab cultures of free-living filamentous heterocystous cyanobacteria (Wolk *et al*., 1976; Ropa *et al*., 2007; Ploug *et al*., 2010). Unique to the results presented here, is that the N transferred along the symbiotic trichome (heterocyst to vegetative cells) is also transferred across the diatom cell membrane.

In terrestrial systems, rapid nutrient transfer is facilitated by the intracellular location of the symbionts within specialized tissues or organs of multicellular hosts, which are connected to the host tissues via vesicles (Rai *et al*., 2000). Nitrogen should be easily transferred from intracellular symbionts, but it is unknown how N transfer is facilitated in these planktonic diatom symbioses.

The orientation of the *Calothrix* heterocyst attached to the intercalary spaces of their *Chaetocoeros* partners may facilitate the transfer of N to the diatom while still exposing the trichome to the surrounding environment (for light and to acquire other nutrients). The efficiencies of nutrient exchange are poorly resolved in most symbioses (Rai *et al.*, 2000), and the mechanisms in these simple unicellular symbioses may be very different from symbiotic systems with multicellular hosts.

As the ^{15}N labeling could be measured on entire individual cells (symbioses), cell-specific rates of N_2 fixation could be calculated for the natural populations (Table 1). Using the ratios obtained from the nanoSIMS analyses, we obtained remarkably similar rates of N_2 assimilation (range, 1.15–71.5 fmol N per cell h^{-1}) amongst all the symbioses, including the unicellular *Crocosphaera* symbionts of *Climacodium* (1.62 fmol N per cell h^{-1}). Our rates were also comparable with the cellular rates previously estimated from bulk N_2-fixation rates for a large expansive mono-specific bloom of *Richelia* associated with *Hemiaulus hauckii* in the North Atlantic Ocean (50 fmol N per cell h^{-1}; Carpenter *et al.*, 1999). This result is surprising given that the symbioses differ in diatom association (that is, *Hemiaulus, Chaetoceros* and *Climacodium*), diatom cell size (1.49×10^3 to 1.56×10^5 μm^3) collection (different ocean basins and during different years), incubation time (30 min–76 h) and cell densities (bloom versus background abundances).

The $^{15}N/^{14}N$ ratios determined on the individual symbiotic cells by nanoSIMS were also used to estimate growth of the symbionts and the diatoms (see Materials and methods). We determined remarkably similar growth rates for all three symbiotic cell types and their respective diatom partners. The estimates of growth rate for the field collected *Hemiaulus* (0.04–0.48 division per day) were similar to those (0.77 division per day) reported for laboratory cultures of another symbiotic diatom, *Rhizosolenia clevi* (Villareal, 1990), which associates with a closely related *Richelia* strain of *Hemiaulus* (Janson *et al.*, 1999; Foster and Zehr, 2006). It should be noted that *R. clevi* are much larger in cell length than the *Hemiaulus* reported here. The other two symbionts, including the unicellular *Crocosphaera* cells associated with *Climacodium*, were also similar (0.38–0.51 per division) to the growth rates of *Richelia*, which was equally surprising given the same reasons aforementioned and additionally, differing cell types of the symbionts (that is, unicellular and heterocystous).

In several of the symbioses (14 of 19) analyzed with nanoSIMS, the estimated growth rates for symbiont and diatom partners were so similar that a synchronous division would be expected (Table 1). In addition, our results indicate that the co-occurring free-living *Richelia* and *Calothrix* cells had substantially reduced growth rate compared with the same symbiont cell types living in association with the diatoms (Table 1). The average rate of N_2 fixation (20.4 and 71.5 fmol N per cell h^{-1}) for the symbiotic heterocystous cells (*Richelia* and *Calothrix*, respectively) is 170–420 times higher than the N_2 fixation rate (0.12 and 0.17 fmol N per cell h^{-1}, respectively) estimated for free-living *Richelia* and *Calothrix* cells (Table 1). In terrestrial symbiotic systems, cyanobionts undergo several structural–functional changes, including modifications to their growth rates and metabolism, which is often coordinated by the host to maximize nutrient transfer and balanced growth amongst the partners (Rai *et al.*, 2000). A similar scenario may exist in these marine symbioses as a means to provide sufficient N for both partners.

As we demonstrated that N was transferred, and growth and N_2 fixation rates were apparently accelerated under symbiotic conditions, we were curious whether the symbionts were fixing more N than required for their growth (see Materials and methods). Assuming similar growth rates for the *Hemiaulus* and the *Richelia*, as was observed in our experiments, we estimate that *Richelia* symbionts fix between 71 and 651% more N than required for their own growth (see Materials and methods). Other cyanobacteria, that is, free-living *Trichodesmium* (Mulholland *et al.*, 2004), also fix more N than required for their own growth, but unique to the symbioses studied here, is that up to 97.3% of the total fixed N is transferred to their diatom partners and not assimilated by the symbionts themselves nor simply released to the environment. Given that N_2 fixation is energetically expensive and highly regulated (Postgate, 1972), we suspect that the diatoms may influence the N metabolism of the symbionts.

Determining the contribution of these fragile associations to global N (and C) has been difficult to predict. We used the cell-specific rates of N_2 fixation determined by nanoSIMS analysis to estimate basin scale N_2 assimilation attributed to the symbioses (see details in Materials and methods). We estimated that the symbiotic diatom populations (0.19 and 0.62 Tmol N per year in Atlantic and Pacific Oceans, respectively) could be an equally important source of new N as the free-living colonial diazotroph, *Trichodesmium* (0.36–0.71 Tmol N per year; Capone *et al.*, 2008), which is usually considered largely responsible for N_2 fixation in the open ocean. The densities of the symbioses are not easily detected and most data on the symbioses are reported during bloom densities, and as we are unable to measure the N release from the symbioses, our estimate is likely an underestimate. Moreover, recent evidence demonstrates that N_2 fixation will be underestimated when the $^{15}N_2$ tracer is introduced as a bubble (Mohr *et al.*, 2010). Although conservative, our calculation reveals the importance of an often un-estimated pool of N, and indicates that diatom symbioses should be included in global N models.

Acknowledgements

A special acknowledgement to Dr F Prahl and Dr A White of OSU (OCE 0726422) and Dr B Popp of UH for inviting and sponsoring RAF on the cruise to Gulf of California. RAF is also grateful to the captains and crew of the R/V New Horizon and R/V Kilo Moana for assistance during sampling in July 2008. RAF and JPZ recognize the helpful suggestions and advice by J Montoya and C Mahaffey in the data processing and D Karl for his helpful suggestions on our manuscript preparation. We also thank two anonymous reviewers for their comments and helpful suggestions. Funding for salary support (RAF) and sample processing has been provided by the National Science Foundation Center for Microbial Oceanography: Research and Education, the Gordon and Betty Moore Foundation (JPZ) and National Science Foundation (RAF and JPZ). The Max Planck Society sponsored the nanoSIMS and irm-MS analyses.

References

Carpenter EJ, Capone DG. (2008). Nitrogen fixation in the marine environment. In: Capone DG, Bronk DA, Mulholland MR, Carpenter EJ (eds) *Nitrogen in the Marine Environment*. Academic Press: London, pp 141–198.

Carpenter EJ, Janson S. (2000). Intracellular symbionts in the marine diatom *Climacodium frauenfeldianum* Grunow. *J Phycol* **36**: 540–544.

Carpenter EJ, Montoya JP, Burns JA, Mulholland M, Subramaniam A, Capone DG. (1999). Extensive bloom of a N_2-fixing diatom/cyanobacterial association in the Tropical Atlantic Ocean. *Mar Ecol Prog Ser* **185**: 273–283.

Clode PL, Stern RA, Marshall AT. (2007). Subcellular imaging of isotopically labeled carbon compounds in a biological sample by ion microprobe (NanoSIMS). *Microsc Res Tech* **70**: 220–229.

Codispoti L. (1995). Is the ocean losing fixed nitrogen? *Nature* **376**: 724.

Finzi-Hart JA, Pett-Ridge J, Weber PK, Popa R, Fallon SJ, Gunderson T *et al.* (2009). Fixation and fate of C and N in the cyanobacterium *Trichodesmium* using nanometer-scale secondary ion mass spectrometry. *Proc Natl Acad Sci USA* **106**: 6345–6350.

Foster RA, O'Mullan GD. (2008). Nitrogen-fixing and nitrifying Symbioses in the marine environment. In: Capone DG, Bronk DA, Mulholland MR, Carpenter EJ (eds). *Nitrogen in the Marine Environment*. Academic Press: London, pp 1197–1218.

Foster RA, Zehr JP. (2006). Characterization of diatom-cyanobacteria symbioses on the basis of *nifH*, *hetR*, and 16S rRNA sequences. *Environ Microbiol* **8**: 1913–1925.

Gruber N. (2005). A bigger nitrogen fix. *Nature* **436**: 786–787.

Gruber N, Sarmiento J. (1997). Global patterns of marine nitrogen fixation and denitrification. *Glob Biogeochem Cycles* **11**: 235–266.

Halm H, Musat N, Lam P, Langlois R, Musat F, Peduzzi S *et al.* (2009). Co-occurrence of denitrification and nitrogen fixation in a meromictic lake, Lake Cadagno (Switzerland). *Environ Microbiol* **11**: 1945–1958.

Janson J, Rai AN, Bergman B. (1995). The intracelllar cyanobiont *Richelia intracellularis* : ultrastructure and immuno-localisation of phycoerythrin, nitrogenase, rubisco, and glutamine synthetase. *Mar Biol* **124**: 1–8.

Janson S, Wouters J, Bergman B, Carpenter EJ. (1999). Host specificity in the *Richelia*-diatom symbioses revealed by *hetR* gene sequence analyses. *Environ Microbiol* **1**: 431–438.

Karl D, Letelier R, Tupas L, Dore J, Christian J, Hebel D. (1997). The role of nitrogen fixation in biogeochemical cycling in the subtropical North Pacific Ocean. *Nature* **388**: 533–538.

Karl D, Michaels A, Bergman B, Capone DG, Carpenter EJ, Letelier R *et al.* (2002). Dinitrogen fixation in the world's oceans. *Biogeochemistry* **57/58**: 47–98.

Lechene CP, Luyten Y, McMahon G, Distel DL. (2007). Quantitative imaging of nitrogen fixation by individual bacteria within animal cells. *Science* **317**: 1563–1566.

Mague T, Weare N, Holm-Hansen O. (1974). Nitrogen fixation in the North Pacific Ocean. *Mar Biol* **24**: 109–119.

Mahaffey C, Michaels AF, Capone DG. (2005). The conundrum of marine N_2 fixation. *Am J Sci* **305**: 546–595.

Michaels A, Olson D, Sarmiento J, Ammerman J, Fanning K, Jahnke R *et al.* (1996). Inputs, losses and transformations of nitrogen and phosphorus in the pelagic North Atlantic Ocean. *Biogeochemistry* **35**: 181–226.

Mohr W, Großkopf T, Wallace DRW, LaRoche J. (2010). Methodological underestimation of oceanic nitrogen fixation rates. *PLoS One* **9**: 1–7.

Montoya J, Holl C, Zehr J, Hansen A, Villareal T, Capone DG. (2004). High rates of N_2 fixation by unicellular diazotrophs in the oligotrophic Pacific Ocean. *Nature* **430**: 1027–1032.

Mulholland M, Bronk DA, Capone DG. (2004). Dinitrogen fixation and release of ammonium and dissolved organic nitrogen by *Trichodesmium* IMS101. *Aquat Microb Ecol* **37**: 85–94.

Musat N, Halm H, Winterholler B, Hoppe P, Peduzzi S, Hillion F *et al.* (2008). A single-cell view on the ecophysiology of anaerobic phototrophic bacteria. *Proc Natl Acad Sci USA* **105**: 17861–17866.

Norris RE. 1961. Observations on phytoplankton organisms collected on the NZOI Pacific Cruise, September 1958. *N Z J Sci* **4**: 162–168.

Ploug H, Musat N, Adam B, Moraru C, Lavik G, Vagner T *et al.* (2010). Carbon and nitrogen fluxes associated with the cyanobacterium *Aphanizomenon* sp. in the Baltic Sea. *ISME J* **4**: 1215–1223.

Postgate J. (1972). *Nitrogen Fixation*. Cambridge University Press: Cambridge, UK.

Rai AN, Söderbäck E, Bergman B. (2000). Cyanobacterium-plant symbioses. *New Phytol* **147**: 449–481.

Redfield AC. (1934). On the proportions of organic derivations in sea water and their relation to the composition of plankton. In: Daniel RJ (ed). *James Johnstone Memorial Volume*. University Press of Liverpool: UK, pp 177–192.

Römer W, Wu TD, Duchambon P, Amessou M, Carrez D, Johannes L *et al.* (2006). Sub-cellular localization of a ^{15}N-labelled peptide vector using NanoSIMS imaging. *Appl Surface Sci* **252**: 6925–6930.

Ropa R, Weber PK, Pett-Ridge J, Finzi JA, Fallon ST, Hutcheon ID *et al.* (2007). Carbon and nitrogen fixation and metabolite exchange in and between individual cells of *Anabaena oscillariodes*. *ISME J* **1**: 354–360.

Stewart WDP. (1973). Nitrogen fixation by photosynthetic microorganisms. *Ann Rev Microbiol* **27**: 283–316.

Strathmann RR. (1967). Estimating the organic carbon content of phytoplankton from cell volume or plasma volume. *Limnol Oceanogr* **12**: 411–418.

Sun J, Liu D. (2003). Geometric models for calculating cell biovolume and surface area for phytoplankton. *J Plank Res* **25**: 1331–1346.

Tomas CR. (1997). *Identifying Marine Phytoplankton*. Academic Press: San Diego, CA, USA.

Venrick E. (1974). The distribution and significance of *Richelia intracellularis* in the North Pacific cdentral gyre. *Limnol Oceanogr* **19**: 437–445.

Villareal T. (1989). Division cycles in the nitrogen-fixing *Rhizosolenia* (Bacillariophyceae) *Richelia* (Nostocaceae) symbiosis. *Br Phycol J* **24**: 357–365.

Villareal T. (1990). Laboratory culture and preliminary characterization of the nitrogen-fixing *Rhizosolenia-Richelia* symbiosis. *Mar Ecol* **11**: 117–132.

Villareal TA. (1994). Widespread occurrence of the *Hemiaulus*-cyanobacteria symbiosis in the southwest North Atlantic Ocean. *Bull Mar Sci* **54**: 1–7.

Wolk CP, Thomas J, Shaffer PW, Austin SM, Galonsky A. (1976). Pathway of nitrogen metabolism after fixation of ^{13}N-labeled nitrogen gas by the cyanobacterium *Anabaena cylindrical*. *J Biol Chem* **251**: 5027–5034.

Zehr JP, Carpenter EJ, Villareal T. (2000). New perspectives on nitrogen-fixing microorganisms in tropical and subtropical oceans. *Trends Microbiol* **8**: 68–73.

Zehr JP, Mellon MT, Zani S. (1998). New nitrogen-fixing microorganisms detected in oligotrophic oceans by amplification of nitrogenase (*nifH*) genes. *Appl Environ Microbiol* **64**: 3444–3450.

Zehr JP, Montoya JP. (2007). Measuring N_2 fixation in the field. In: Bothe H, Ferguson SJ, Newton WE. (eds). *Biology of the Nitrogen Cycle*. Elsevier: Amsterdam, The Netherlands, pp 193–205.

This work is licensed under the Creative Commons Attribution-NonCommercial-No Derivative Works 3.0 Unported License. To view a copy of this license, visit http://creativecommons.org/licenses/by-nc-nd/3.0/